J. Fluid Mech. (1991), *vol.* 229, *pp.* 517–529
Printed in Great Britain

Instabilities of longitudinal rolls in the presence of Poiseuille flow

By R. M. CLEVER AND F. H. BUSSE

Institute of Geophysics and Planetary Physics, University of California at Los Angeles, CA 90024, USA *and* Institute of Physics, University of Bayreuth, 858 Bayreuth, Germany

(Received 6 August 1990)

Longitudinal rolls represent the preferred form of convection in a horizontal fluid layer heated from below in the presence of parallel shear flows for sufficiently low Reynolds numbers and for a finite range of the Rayleigh number above the critical value Ra_c. In this paper properties of the longitudinal rolls and their stability with respect to three-dimensional disturbances are investigated in the case of Poiseuille flow. While the convective heat transport is independent of the Reynolds number, the mass flux through the channel at a given Reynolds number decreases with increasing Rayleigh number. A wavy instability is found to set in at a finite Reynolds number and relatively low Rayleigh numbers, depending on the Prandtl number P. In particular, the stability region for longitudinal rolls is analysed for $P = 0.025$, 0.1, 0.71, 2.5, and 7. For sufficiently small Reynolds number the oscillatory, the skewed varicose or the knot instability can precede the wavy instability. For $P = 7$ the wavy instability is preceded by a modified knot instability throughout the Reynolds-number range that has been investigated. In spite of the difference in symmetry, the results for Poiseuille flow resemble those obtained earlier in the case of plane Couette flow.

1. Introduction

Longitudinal rolls aligned with the direction of the mean shear have long been recognized as a preferred form of convection in a horizontal fluid layer heated from below and in the presence of a mean flow. Early experiments by Idrac and Terada as reported by Avsec & Luntz (1937) dealt with this situation, and many applications from cloud streets in the atmosphere (Bénard & Avsec, 1938; Kuettner 1971; Brown 1980) to problems of heat transfer in the engineering sciences have been considered. For a review of this and other work refer to Kelly (1977).

Longitudinal rolls compete with hydrodynamically excited transverse waves at the onset of instability of the horizontally uniform basic state. In the case of Poiseuille flow longitudinal rolls represent the preferred mode of instability at the Rayleigh number $Ra_c = 1708$ for Reynolds numbers less than about $Re_c = 5400$ according to linear theory (Gage & Reid 1968). In the case of plane Couette flow no hydrodynamic instability is predicted by linear theory and the onset of instability thus occurs solely in the form of longitudinal convection rolls. For the case of combined Poiseuille and Couette flow see the recent paper of Fujimura & Kelly (1988). Experiments show that finite-amplitude instabilities typically occur for Reynolds numbers above threshold values of 10^3 and linear theory is thus of little physical relevance at high Reynolds number. For this reason only Reynolds numbers of the order 10^3 or less will be considered in this paper.

Longitudinal convection rolls are governed by the same equations as two-dimensional rolls in the absence of a shear flow. The Nusselt number is thus independent of the Reynolds number and this property also holds for the velocity components perpendicular to the direction of the mean flow. The latter is strongly affected by the action of the convection rolls, at least for low Prandtl numbers, and much of the theoretical research has therefore focused on the velocity component in the mean flow direction (see, for example, Ogura & Yagihashi 1969; Hwang & Cheng, 1971).

The stability of longitudinal rolls in the presence of Poiseuille flow has not been studied until now, however, even though evidence for the wavy instability of longitudinal rolls has been available since the observations discussed by Avsec & Luntz (1937) and by Avsec (1937). The analysis of this paper aims to close this gap and to provide results analogous to those obtained in the case of Couette flow by Clever, Busse & Kelly (1977). The major conclusion of the following analysis is that the wavy instability severely restricts the region of the physical realizability of longitudinal rolls. Because the interaction between convection and the mean shear increases through the transition, amplitude-sensitive properties of the wavy rolls such as the Nusselt number tend to increase less rapidly with Rayleigh number than in the case of longitudinal rolls.

The paper starts with the mathematical formulation of the problem in §2. In §3 some of the properties of steady longitudinal rolls will be considered. The main results of the paper on the wavy instability are presented in §4. Concluding remarks and an outlook on further work are offered in §5.

2. Mathematical formulation

We consider a horizontal fluid layer of depth d with rigid upper and lower boundaries which are kept at the temperatures T_1 and T_2, respectively. A uniform pressure gradient in the direction of the horizontal unit vector $\boldsymbol{i}$ is applied, such that a mean flow with a parabolic profile is realized as the basic state of the problem. Using d as lengthscale, d^2/ν as timescale (where ν is the kinematic viscosity of the fluid) and $(T_2-T_1)P$ as temperature scale, we write the equations of motion for the velocity vector $\boldsymbol{v}$ and the heat equation for the deviation ϑ of the temperature field from the state of pure conduction in the dimensionless form

$$\nabla^2\boldsymbol{v}+\boldsymbol{k}Ra\,\vartheta-\nabla\pi=\boldsymbol{v}\cdot\nabla\boldsymbol{v}+\partial/\partial t\,\boldsymbol{v}, \tag{2.1a}$$

$$\nabla\cdot\boldsymbol{v}=0, \tag{2.1b}$$

$$\nabla^2\vartheta+\boldsymbol{k}\cdot\boldsymbol{v}=P(\boldsymbol{v}\cdot\nabla\vartheta+\partial/\partial t\,\vartheta), \tag{2.1c}$$

where the Rayleigh number Ra and the Prandtl number P are defined by

$$Ra=\frac{\gamma g(T_2-T_1)\,d^3}{\nu\kappa},\quad P=\frac{\nu}{\kappa}.$$

The thermal expansivity is denoted by γ, κ is the thermal diffusivity and g is the acceleration of gravity, which is directed opposite to the unit vector $\boldsymbol{k}$. All terms that can be written as gradients in equation (2.1a) have been combined into $\nabla\pi$. We shall use a Cartesian system of coordinates with the z-coordinate in the direction of $\boldsymbol{k}$ and the x-coordinate parallel to $\boldsymbol{i}$.

The basic state of the system is described by

$$\boldsymbol{v} = i u_0 \equiv Re\,(1-4z^2)\,\boldsymbol{i}, \quad \vartheta = 0, \tag{2.2}$$

where the Reynolds number

$$Re = \frac{u_{0\max} d}{\nu}$$

is defined with the maximum value of the parabolic velocity profile. Since the velocity field is solenoidal we introduce the representation

$$\boldsymbol{v} = (u_0 + u_1)\,\boldsymbol{i} + \check{\boldsymbol{v}},$$

with
$$\check{\boldsymbol{v}} \equiv \nabla \times (\nabla \times \boldsymbol{k}\varphi) + \nabla \times \boldsymbol{k}\psi \equiv \boldsymbol{\delta}\varphi + \boldsymbol{\varepsilon}\psi \tag{2.3}$$

for the description of the secondary motions after the onset of convection, where the average of the scalar functions φ and ψ over horizontal planes is assumed to vanish such that the mean flow is described solely by $\boldsymbol{i}(u_0 + u_1)$.

By taking the vertical components of the curl and of the curlcurl of (2.1 *a*) we obtain the following equations for φ and ψ:

$$\nabla^4 \Delta_2 \varphi - Ra\,\Delta_2 \vartheta = \boldsymbol{\delta} \cdot (\check{\boldsymbol{v}} \cdot \nabla \check{\boldsymbol{v}}) + \left[(u_0 + u_1)\frac{\partial}{\partial x} + \frac{\partial}{\partial t}\right] \nabla^2 \Delta_2 \varphi - (u_0'' + u_1'')\frac{\partial}{\partial x}\Delta_2 \varphi, \tag{2.4a}$$

$$\nabla^2 \Delta_2 \psi = \boldsymbol{\varepsilon} \cdot (\check{\boldsymbol{v}} \cdot \nabla \check{\boldsymbol{v}}) + \left[(u_0 + u_1)\frac{\partial}{\partial x} + \frac{\partial}{\partial t}\right] \Delta_2 \psi - (u_0' + u_1')\frac{\partial}{\partial y}\Delta_2 \varphi, \tag{2.4b}$$

where the prime denotes the differentiation with respect to z and Δ_2 represents the two-dimensional Laplacian, $\Delta_2 = \partial^2/\partial x^2 + \partial^2/\partial y^2$. For a complete system of equations we must add an equation for u_1 by taking the horizontal average (indicated by a bar) of the x-component of (2.1 *a*):

$$\left(\frac{\partial^2}{\partial z^2} - \frac{\partial}{\partial t}\right) u_1 = -\frac{\partial}{\partial z}\left(\overline{\Delta_2 \varphi \left(\frac{\partial^2}{\partial x\,\partial z}\varphi + \frac{\partial}{\partial y}\psi\right)}\right) \tag{2.4c}$$

We also rewrite equation (2.1 *c*) for ϑ,

$$\nabla^2 \vartheta - \Delta_2 \varphi = P\left(\check{\boldsymbol{v}} \cdot \nabla \vartheta + (u_0 + u_1)\frac{\partial}{\partial x}\vartheta + \frac{\partial}{\partial t}\vartheta\right). \tag{2.4d}$$

The corresponding boundary conditions are given by

$$\varphi = \partial/\partial z \varphi = \psi = \vartheta = u_1 = 0, \quad \text{at} \quad z = \pm\tfrac{1}{2} \tag{2.5}$$

Steady longitudinal convection rolls are described by x-independent solutions of (2.4). In this case ψ, u_0 and u_1 do not enter (2.4 *a*) and (2.4 *b*) and the solutions $\varphi(y, z)$, $\vartheta(y, z)$ are thus independent of the Reynolds number. For the variables ψ and u_1 the following linear system of equations is obtained:

$$\nabla^2 \frac{\partial}{\partial y}\psi = \boldsymbol{\delta}\varphi \cdot \nabla \frac{\partial}{\partial y}\psi - (u_0' + u_1')\,\Delta_2 \varphi, \tag{2.6a}$$

$$\frac{\partial^2}{\partial z^2} u_1 = -\frac{\partial}{\partial z}\overline{\Delta_2 \varphi \frac{\partial}{\partial y}\psi}. \tag{2.6b}$$

For the actual solution of the problem we employ the Galerkin method in which

the dependent variables are expanded in complete systems of functions satisfying the respective boundary conditions. The steady longitudinal roll solution is described by

$$\varphi = \sum_{l,n} a_{ln} \cos l\alpha y f_n(z), \tag{2.7a}$$

$$\vartheta = \sum_{l,n} b_{ln} \cos l\alpha y \sin n\pi(z+\tfrac{1}{2}), \tag{2.7b}$$

$$\psi = \sum_{l,n} c_{ln} \sin l\alpha y \sin n\pi(z+\tfrac{1}{2}), \tag{2.7c}$$

$$u_1 = \sum_{n} U_n \sin n\pi(z+\tfrac{1}{2}), \tag{2.7d}$$

where the functions $f_n(z)$ are the same as those used by Clever & Busse (1974, 1981, 1987) in the analysis of convection rolls without shear flow. We also note that the solutions of interest exhibit vanishing coefficients whenever $l+n$ is an odd integer in (2.7*a*, *b*) and coefficients with even $l+n$ and with even n vanish in (2.7*c*) and (2.7*d*), respectively.

The stability of steady solutions of the form (2.7) is studied by the superposition of three-dimensional infinitesimal disturbances,

$$\tilde{\varphi} = \sum_{l,n} (\hat{a}_{ln} \cos l\alpha y + \check{a}_{ln} \sin l\alpha y) f_n(z) \exp\{\mathrm{i}bx + \mathrm{i}dy + \sigma t\}, \tag{2.8}$$

with analogous expressions for $\tilde{\vartheta}$ and $\tilde{\psi}$. Since the disturbances of interest have finite values of b, the horizontal mean of the flow disturbance is zero.

While expression (2.8) represents general disturbances, all instabilities to be considered in the following correspond to the case $d = 0$ except for the skewed varicose instability. In the case $d = 0$ the disturbances of the form (2.8) separate into two classes, those with vanishing coefficients $\hat{a}_{ln}$ and those with vanishing coefficients $\check{a}_{ln}$. Since the separation into two classes leads to a considerable decrease in the amount of computation, and since the onset of the skewed varicose instability can be estimated from earlier results in the small region of the parameter space where it is relevant, we shall use the property $d = 0$ in the following.

In the numerical computations of longitudinal roll solutions and in the stability analysis the summations in expressions (2.7), (2.8) must be truncated. As in previous work we neglect all coefficients with subscripts l, n satisfying the inequality

$$l+n > N_{\mathrm{T}},$$

where N_{T} can be varied in order to test the accuracy of the approximation. Most of the results displayed in the figures of this paper have been obtained with both $N_{\mathrm{T}} = 8$ and $N_{\mathrm{T}} = 10$. Typically the results differ by less than 1 %. At the highest Rayleigh numbers only this difference grows to a few percent and some cases have been computed with $N_{\mathrm{T}} = 12$.

3. Interaction of longitudinal rolls with the mean flow

Most of the properties of steady longitudinal convection rolls such as the Nusselt number and the y- and z-components of the velocity field remain unchanged in the presence of a mean shear in the x-direction. We thus can refer to earlier computations of properties of convection rolls given by Busse (1967), Clever & Busse (1974, 1981),

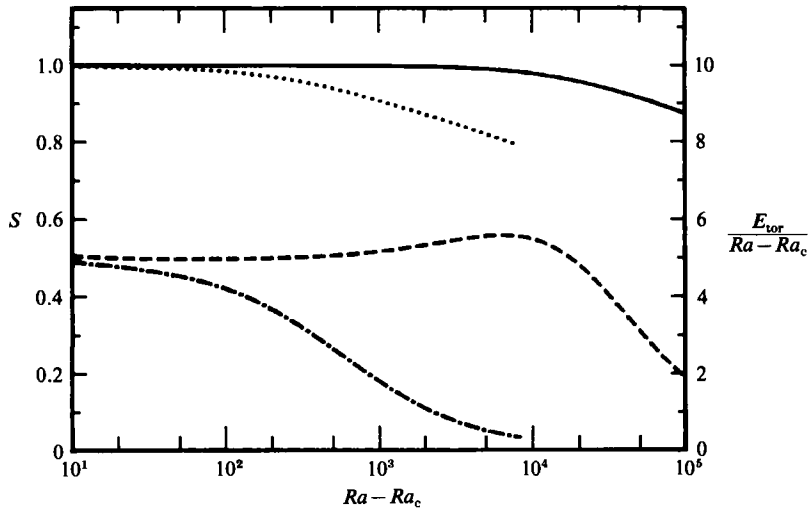

FIGURE 1. The ratio S of the mass fluxes with convection and without convection as function of Ra–Ra_c for $P = 7.0$ (solid line) and $P = 0.71$ (dotted line). Also shown is the kinetic energy E_{tor} of the fluctuating x-component of the velocity field for $P = 7.0$ (dashed line) and $P = 0.71$ (dashed–dotted line). In all cases $Re = 1000$ and $\alpha = 3.117$ have been used.

Schneck & Veronis (1967) and others. Here we are especially interested in the changes in the longitudinal components of the velocity field introduced by the convection flow. Some of these changes have been studied by Ogura & Yagihashi (1969) and by Hwang & Cheng (1971) in the case of air. In the following we shall provide some additional information for $P = 0.71$ and consider other Prandtl numbers.

One of the most interesting changes introduced by the onset of convection is the decrease in the mass flux through the layer at a fixed mean pressure gradient. The dimensionless mass flux corresponding to Poiseuille flow is given by $\langle u_0 \rangle = \frac{2}{3}Re$, where the angular brackets indicate the average over the fluid layer. The ratio S of the mass flux in the presence of longitudinal rolls divided by the mass flux of Poiseuille flow is given by

$$S = 1 + \tfrac{3}{2}\langle u_1 \rangle / Re \tag{3.1}$$

and has been plotted for two typical cases in figure 1 as function of the Rayleigh number. As is evident from the curves, the effect of convection decreases with increasing Prandtl number. The decrease in the mass flux is connected with the fact that the work done by the pressure gradient is no longer balanced solely by the dissipation caused by the viscous stress of the mean velocity field. Instead the dissipation associated with the fluctuating component makes a significant contribution. By multiplying (2.6a) by $\partial\psi/\partial y$ and averaging it over the fluid layer we obtain the relationships

$$\langle |\nabla \partial/\partial y\, \psi|^2 \rangle = \langle (u_0' + u_1')\, \overline{\Delta_2 \varphi\, \partial/\partial y\, \psi} \rangle = -\langle (u_0' + u_1')\, u_1' \rangle \tag{3.2}$$

where the integrated version of (2.6b) and the property that u_1'' is symmetric in z have been used. Relationships (3.2) can be rewritten in the form

$$\langle |\nabla \partial/\partial y\, \psi|^2 \rangle + \langle |u_0' + u_1'|^2 \rangle = \langle u_0'(u_0' + u_1') \rangle = \langle u_0''(u_0 + u_1) \rangle, \tag{3.3}$$

where the right-hand side expresses the work done by the pressure gradient while the left-hand side describes the viscous dissipation associated with the longitudinal velocity component. Because of the relationship

$$2\langle u_0' u_1' \rangle / Re = -\langle z u_1' \rangle = \langle u_1 \rangle,$$

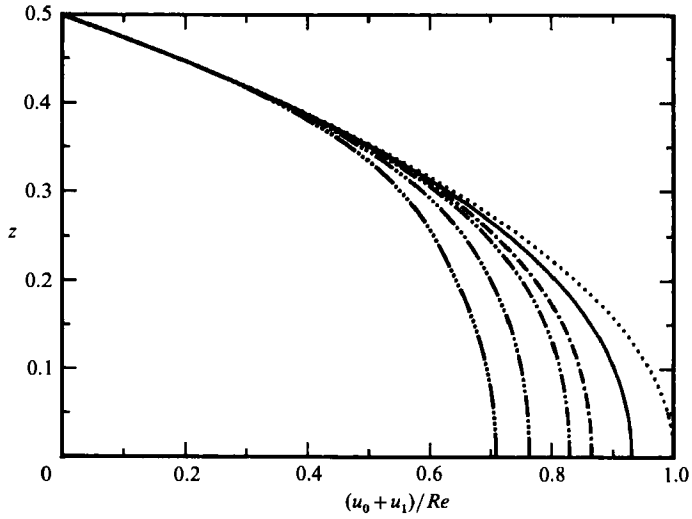

FIGURE 2. The profiles of the mean flow for the case $P = 0.71$, $Re = 20$ for the Rayleigh numbers (from right to left) $Ra = 0$, 2000, 2500, 3000, 5000, 10^4. Because of the symmetry about the plane $z = 0$, only the upper half has been shown.

the quantity S can also be expressed in the form

$$S = 1+\langle u_1\rangle/\langle u_0\rangle = 1-2(\langle|\nabla\partial/\partial y|^2\rangle+\langle|u_1'|^2\rangle)/Re \tag{3.4}$$

which relates the decrease in the mass flux to the shift in the dissipation. We have also plotted in figure 1 the kinetic energy of the fluctuating x-component of the velocity field

$$E_{\rm tor} \equiv \tfrac{1}{2}\langle|\nabla\partial/\partial y\,\psi|^2\rangle \tag{3.5}$$

which grows roughly proportional to Ra–Ra_c. We use the term 'toroidal' for the component of the velocity field described by ψ. The component described by φ will be called 'poloidal'.

The reduction of the mean flow amplitude due to the influence of convection is shown in figure 2. Since the mean shear at the boundaries remains constant for a given value Re, the decrease of the mean flow is associated with a flattening of the profile. With increasing Rayleigh number, the effect of convection on the mean flow tends to saturate such that little change is noticed as the Rayleigh number grows to the order 10^4.

4. Instabilities of longitudinal rolls

Predominant among the instabilities of longitudinal rolls in the presence of a mean shear is the wavy instability. It corresponds to growing disturbances of the form (2.8) with vanishing d and vanishing coefficients $\hat{a}_{ln}$. The dependence of the real part σ_r of the growth rate σ on the longitudinal wavenumber b is such that the instability first sets in with vanishingly small values of b as the Rayleigh number is increased. Beyond the stability boundary the value of b corresponding to a maximum growth increases rapidly as is shown in figure 3. The imaginary part σ_i reflects the advection of the disturbances by the mean flow. Thus σ_i is approximately proportional to b and to the Reynolds number. In fact, the relationship

$$\sigma_i \approx b\langle u_0+u_1\rangle \tag{4.1}$$

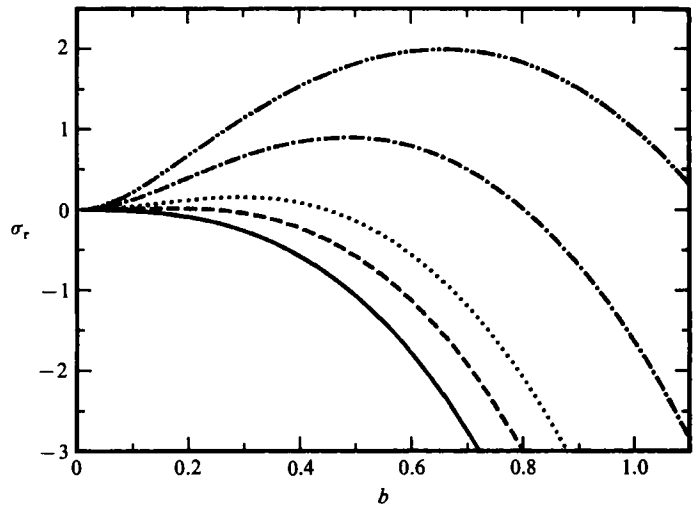

FIGURE 3. The real part σ_r of the growth rate as a function of the wavenumber b for the Rayleigh numbers 3000, 2600, 2300, 2200, 2100 (from top to bottom) for the case $P = 0.71$, $Re = 200$, $\alpha = 3.117$.

based on the z-average of the mean flow appears to be valid within a few percent throughout the parameter space.

In order to gain an impression of the wavy instability of longitudinal rolls, computations at a Rayleigh number above the critical value Ra_{II} have been carried out based on an analysis analogous to that described for the oscillatory instability by Clever & Busse (1987). Because the oscillatory instability of convection rolls exhibits the same symmetry properties as the wavy instability, only minor changes were required in the computer program. As an example we show the way longitudinal roll in figure 4. The temperature distribution (figure 4*a*) clearly indicates that the waviness represents an alternating shift of the roll structure towards the left and the right of the mean flow direction. The shift is the result of the advection by a y-independent component of motion which is described by the y-independent part of $-\partial\bar{\psi}/\partial x$. Besides this latter component a component proportional to $\sin 2\alpha y$ can be seen in figure 4(*b*) while the $\sin\alpha y$-component of ψ vanishes at $z = 0$ for reasons of symmetry. Away from the mid-plane the $\sin\alpha y$-component of ψ predominates as can be seen in figure 4(*c*).

A typical example of the stability boundary introduced by the wavy instability is shown in figure 5 in the case of $P = 0.1$. Evidently the stability boundary depends little on the Reynolds number once the latter has exceeded a threshold value. Using the same arguments presented in the case of an inclined convection layer (Clever & Busse, 1977) and for convection in the presence of Couette flow (Clever *et al.* 1977) we can derive the approximate relationship

$$\sigma_r = -b^2\{Re^2(A-(Ra-Ra_c)B)+(Ra-Ra_c)C+\ldots\} \tag{4.2}$$

for the real part of the growth rate of the wavy instability. Instead of a formal mathematical derivation of this expression we briefly repeat the arguments leading to relationship (4.2). Since the instability may be regarded as a modification of the neutral perturbation in the form of a translation of the longitudinal roll pattern, σ_r must vanish for $b = 0$. Because the onset of oblique rolls requires a Rayleigh number which is of the order b^2Re^2 higher than the critical value Ra_c (at least for Reynolds

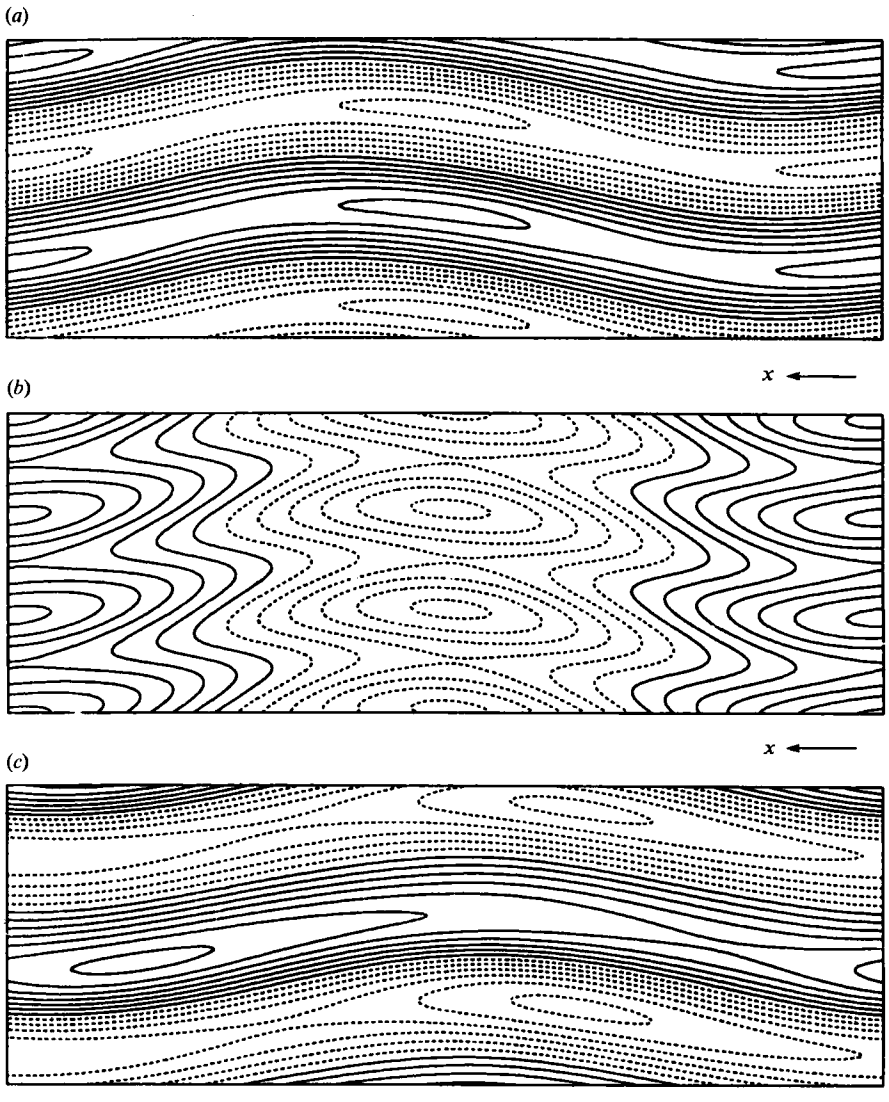

FIGURE 4. (a) Isotherms in the plane $z = 0$ for wavy longitudinal rolls and lines of constant ψ in the planes $z = 0$, (b), and $z = -0.3$, (c). Parameter values are $Ra = 3000$, $P = 0.71$, $Re = 200$, $\alpha_x = 0.7$, $\alpha_y = 3.117$.

numbers less than 5×10^3) the coefficient A must be positive. Another stabilizing influence arises from finite-amplitude properties of the rolls even in the absence of a shear flow. In the latter case the wavy instability corresponds to the zigzag instability which can occur only for wavenumbers α sufficiently smaller than α_c. For reasons of symmetry the relevant terms are proportional to the square of the amplitude of convection, and we thus conclude that the coefficient C in expression (4.2) is positive. The wavy instability is caused by terms involving the toroidal component of motion which give rise to the terms proportional to B at leading order. The expression

$$Ra_{II} - Ra_c \approx Re^2 A[C - Re^2 B]^{-1} \tag{4.3}$$

for the stability boundary $Ra_{II}(Re)$ derived from expression (4.2) appears to describe quite well the numerical results for moderate values of Re and Ra_{II}.

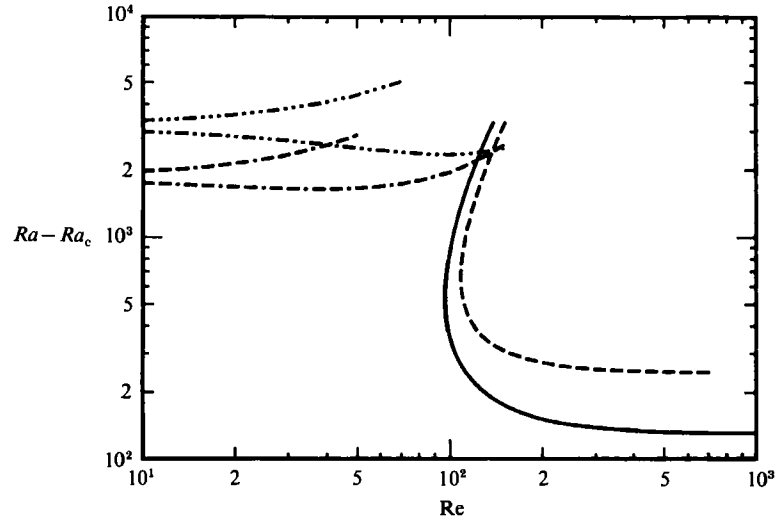

FIGURE 5. The stability boundaries of longitudinal rolls as function of the Reynolds number Re and the Rayleigh number Ra for $P = 0.1$. Rolls are unstable above and to the right of the solid (wavy instability) and the double dash–dotted lines in the case $\alpha = 3.117$. The corresponding lines in the case $\alpha = 2.6$ are given by the dashed and the dash–double dotted lines. The triple dash–dotted and the dash–triple dotted lines indicate the second eigenvalue of the oscillatory instability corresponding to waves travelling in the direction of the mean flow.

At low Reynolds numbers the wavy instability disappears and is replaced by instabilities of convection rolls in the absence of a mean shear. A typical instability of this kind at low Prandtl numbers is the oscillatory instability. It is of interest to consider the influence of the mean flow on the oscillatory instability. As is evident from figure 5 and 6, the double eigenvalue of the growth rate at $Re = 0$ splits into two in the presence of Poiseuille flow since the two travelling wave modes are no longer equivalent. The wave travelling in the direction opposite to the mean flow becomes the preferred mode of oscillatory instability. Because the phase speed and the advection by the mean flow have opposite signs, the imaginary part σ_i of the growth rate for the latter actually goes through zero at a Reynolds number of about 30. The value for $\alpha = 3.117$ is a bit higher, for $\alpha = 2.6$ a bit lower, than 30, in both the cases $P = 0.1$ and $P = 0.7$. The preferred wavenumber b of the oscillatory instability also varies along the two branches of travelling waves. b increases from 2.5 to 3.2 along the lower branches and decreases from 2.4 to 1.7 along the upper branch in figure 6. This variation is somewhat less pronounced in the case of figure 5. It should be noted that at Prandtl numbers of order unity, as in the case of air shown in figure 6, the oscillatory instability is preceded by the skewed varicose instability, at least for wavenumbers α in excess of 2.3. Because the latter instability corresponds to a finite ratio of the parameters d and b in (2.8) its stability boundary has not been calculated in the present analysis. In analogy to the oscillatory instability we expect that the Rayleigh number for onset of the skewed varicose instability changes relatively little from its value at $Re = 0$ in the range $Re \lesssim 10^2$ where it will be relevant. Since longitudinal convection rolls are stable at supercritical Rayleigh numbers for a finite range of wavenumbers α which typically tends to shift to lower values of α with increasing Rayleigh number, we have selected a lower value of α in addition to the critical value $\alpha_c = 3.117$. The stability properties of the longitudinal rolls depend rather smoothly on the wavenumber α and approximate results for intermediate

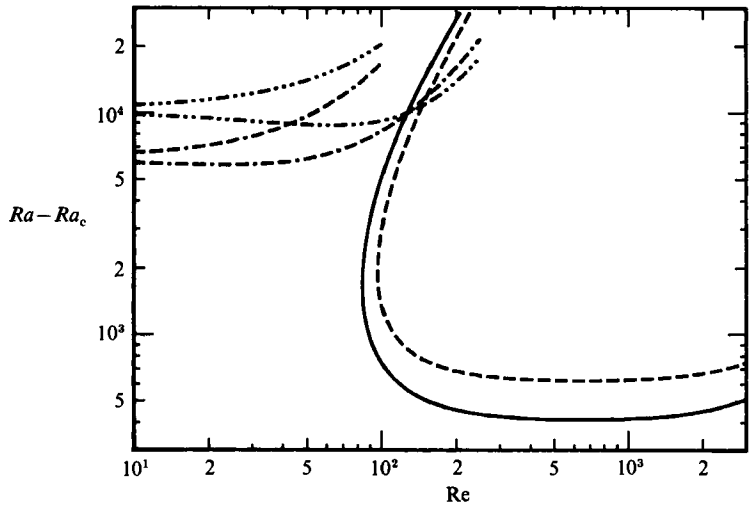

FIGURE 6. The same as figure 5 for the case of $P = 0.7$. At low Reynolds number the skewed varicose instability (Busse & Clever, 1979) precedes the onset of the oscillatory instability. The corresponding boundary has not been plotted.

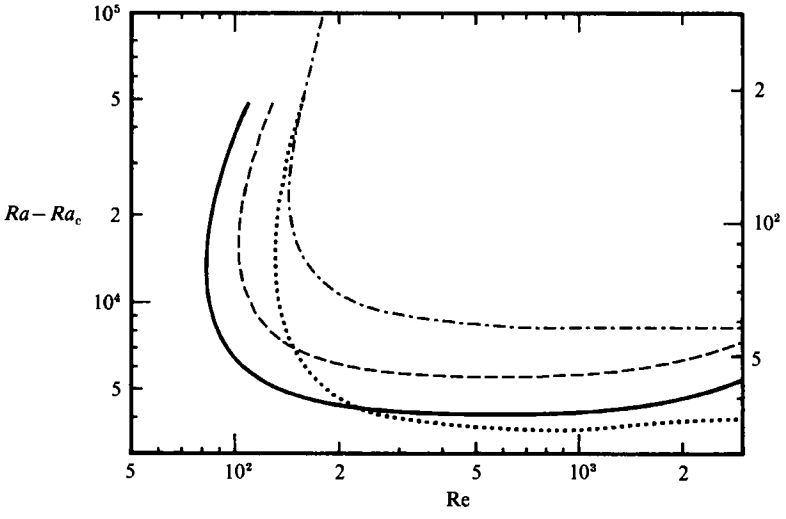

FIGURE 7. The stability boundaries corresponding to the onset of the wavy instability in the cases $P = 2.5$ (left ordinate) for $\alpha = 3.117$ (solid line) and for $\alpha = 2.6$ (dashed line) and in the case $P = 0.025$ (right ordinate) for $\alpha = 3.117$ (dotted line) and $\alpha = 2.9$ (dash–dotted line).

wavenumbers can be obtained by interpolation from the curves displayed in figures 5–8.

The minimum Reynolds number for the onset of the wavy instability changes relatively little as the Prandtl number is varied. But the minimum of the Rayleigh number for onset varies strongly with P. The difference between the critical Rayleigh number Ra_{II} for the wavy instability and the critical Rayleigh number Ra_c for the onset of longitudinal rolls increases in proportion to P. In other words, the parameter A in (4.3) is roughly proportional to the Prandtl number, while B and C are independent of it. The region of stable rolls is thus decreased dramatically in the case of mercury shown in figure 7. With increasing Prandtl number the influence of the mean flow diminishes. In the case $P = 2.5$ which is also shown in figure 7 the wavy

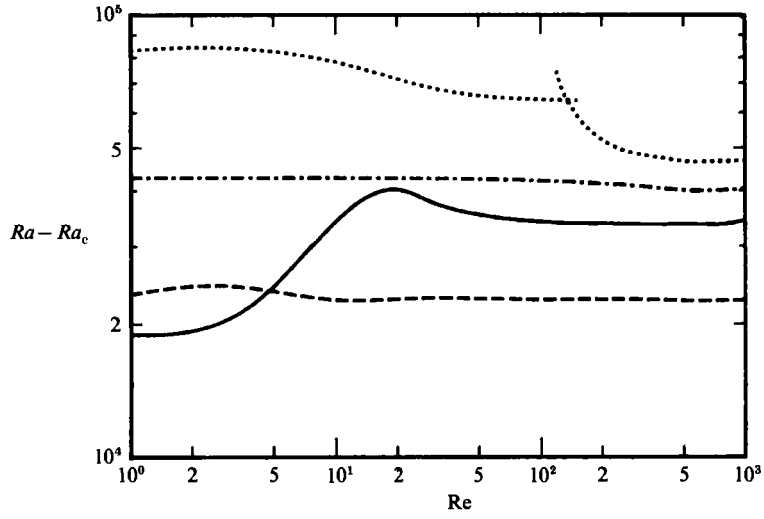

FIGURE 8. Stability boundaries of longitudinal rolls as a function of Rayleigh and Reynolds numbers in the case $P = 7$. The knot instability occurs in the region above the solid line (for $\alpha = 3.117$) and above the dashed line (for $\alpha = 2.2$). The onset of the oscillatory and wavy instabilities correspond to the dotted line for $\alpha = 3.117$ and to the dash–dotted line for $\alpha = 2.2$. See text for a more detailed description.

instability still precedes other instabilities, but in the case of water shown in figure 8 the knot instability occurs first when the Rayleigh number is increased. The latter instability also appears to be rather insensitive to the Reynolds number except for low values of Re. But the wavenumber b along the roll axis decreases roughly with the inverse of the Reynolds number.

Although the wavy instability exhibits the same symmetry properties as the oscillatory instability of convection rolls (Busse 1972; Clever & Busse 1974), the eigenvalues are usually well separated. The dotted line in figure 8 shows the replacement of the oscillatory instability by the wavy instability at a Reynolds number of about 120. While the wavy instability is characterized by imaginary parts σ_i of the growth rate given approximately by relationship (4.1), the oscillatory instability corresponds to a period which is given by the circulation time of particles in a convection roll and thus is nearly independent of b except for the effects of advection by the mean flow. In the case $\alpha = 2.2$ of figure 8 the dash-dotted line describes the onset of the oscillatory instability according to this distinction.

5. Concluding remarks

The wavy instability of longitudinal rolls in the presence of Poiseuille flow is clearly evident in some of the pictures of experimental observations shown in the papers by Avsec (1937) and Avsec & Luntz (1937). Since quantitative data have not been provided for those experiments and because they also do not seem to be available from later experiments, we are not able to compare the theoretical predictions for the onset of the wavy instability with the observations. Since the laboratory realization of convection rolls in the presence of Poiseuille flow is relatively straightforward, we hope that our computations will stimulate more experiments.

The form of the stability boundary in a Ra–Re diagram for Poiseuille flow is

surprisingly similar to that for Couette flow (Clever *et al.* 1977) at least for $P = 0.71$ which is the only case treated in the latter paper. For reasons of symmetry the fields ψ, $\tilde{\psi}$ have vanishing coefficients c_{ln} for odd $l+n$ instead of even $l+n$ in the latter case and the growth rate for the wavy disturbances is real. These differences do not seem to affect the mechanism of instability, however.

The properties of the longitudinal rolls in the presence of Poiseuille flow remain unchanged when a homogeneous longitudinal magnetic field is imposed in the case of an electrically conducting fluid. But the wavy instability and other three-dimensional instabilities are likely to be delayed by the stabilizing influence of the Lorentz force. A similar influence will be exerted by the Coriolis force in a rotating system with the axis of rotation coincident with the direction of the mean flow. This situation may be realized in the thin gap between rigidly rotating cylinders with the centrifugal force providing the effective gravity. The properties displayed in figure 1 and 2 are thus of interest for Rayleigh numbers higher than the values Ra_{II} calculated in this paper.

It will be of interest to analyse the properties of the wavy longitudinal rolls generated by the growth of the wavy instability. Some preliminary computations of finite-amplitude wavy rolls such as those displayed in figure 4 indicate that the convective heat transport is reduced significantly by the evolution of the three-dimensional wavy pattern. It is planned to address the problem of the dependence of finite-amplitude wavy rolls in the various dimensionless parameters in future work.

The research reported in this paper has been supported by the Atmospheric Sciences Section of the US National Science Foundation.

REFERENCES

AVSEC, D 1937 Sur les formes ondulées des tourbillons en bandes longitudinales. *C. R. Acad. Sci. Paris* **204**, 167–169.

AVSEC, D. & LUNTZ, M. 1937 Tourbillons, thermoconvectifs et electroconvectifs. *La Météorologie* **31**, 180–194.

BÉNARD, H. & AVSEC, D. 1938 Travaux récents sur les tourbillons cellulaires et les tourbillons en bandes, applications á l'astrophysique et la météorologie. *J. Phys. Radium* (7) **9**, 486–500.

BROWN, R. A. 1980 Longitudinal instabilities and secondary flows in the planetary boundary layer: a review. *Rev. Geophys. Space Phys.* **18**, 683–697.

BUSSE, F. H. 1967 On the stability of two-dimensional convection in a layer heated from below. *J. Math Phys.* **46**, 140–150.

BUSSE, F. H. 1972 The oscillatory instability of convection rolls in a low Prandtl number fluid. *J. Fluid Mech.* **52**, 97–112.

BUSSE, F. H. & CLEVER, R. M. 1979 Instabilities of convection rolls in a fluid of moderate Prandtl number. *J. Fluid Mech.* **91**, 319–335.

CLEVER, R. M. & BUSSE, F. H. 1974 Transition to time-dependent convection. *J. Fluid Mech.* **65**, 625–649.

CLEVER, R. M. & BUSSE, F. H. 1977 Instability of longitudinal convection rolls in an inclined layer. *J. Fluid Mech.* **81**, 107–127.

CLEVER, R. M. & BUSSE, F. H. 1981 Low Prandtl number convection in a layer heated from below. *J. Fluid Mech.* **102**, 61–74.

CLEVER, R. M. & BUSSE, F. H. 1987 Nonlinear oscillatory convection. *J. Fluid Mech.* **176**, 403–417.

CLEVER, R. M., BUSSE, F. H. & KELLY, R. E. 1977 Instabilities of longitudinal convection in Couette flow. *Z. Angew. Math. Phys.* **28**, 771–783.

FUJIMURA, K. & KELLY, R. E. 1988 Stability of unstable stratified shear flow between parallel plates. *Fluid Dyn. Res.* **2**, 281–292.

GAGE, N. S. & REID, W. H. 1968 The stability of thermally stratified plane Poiseuille flow. *J. Fluid Mech.* **33**, 21–32.

HWANG, G. I. & CHENG, K. C. 1971 A boundary vorticity method for finite amplitude convection in plane Poiseuille flow. *Developments in Mechanics, vol.* 6, *Proc. 12th Midwestern Mech. Conf.*, pp. 207–220.

KELLY, R. E. 1977 The onset and development of Rayleigh–Bénard convection in shear flows: A review. In *Physiochemical Hydrodynamics* (ed. D. B. Spalding), pp. 65–79. Advance Publications.

KUETTNER, J. P. 1971 Cloud bands in the Earth's atmosphere. *Tellus* **23**, 404–425.

OGURA, Y. & YAGIHASHI, A. 1969 A numerical study of convection rolls in a flow between horizontal parallel plates. *J. Met. Soc. Japan* **47**, 205–217.

SCHNECK, P. & VERONIS, G. 1967 Comparison of some recent experimental and numerical results in Bénard convection. *Phys. Fluids* **10**, 927–930.